

Effect of Changing Molecular End Groups on Surface Properties: Synthesis and Characterization of Poly(styrene-*b*-semifluorinated isoprene) Block Copolymers with $-\text{CF}_2\text{H}$ End Groups

Teruaki Hayakawa,[‡] Jianguo Wang,^{†,^} Maoliang Xiang,^{†,§} Xuefa Li,[†] Mitsuru Ueda,[‡] Christopher K. Ober,^{*,†} Jan Genzer,[§] Easan Sivaniah,[‡] Edward J. Kramer,^{‡,‡} and Daniel A. Fischer^{‡,‡}

Materials Science and Engineering, Cornell University, Ithaca, New York 14853-1501; Human Sensing and Functional Sensor Engineering, Graduate School of Engineering, Yamagata University, Yonezawa, Yamagata 992, Japan; Department of Chemical Engineering, NCSU, Raleigh, North Carolina; Department of Materials, UCSB, Santa Barbara, California 93106; Department of Chemical Engineering, UCSB, Santa Barbara, California 93106; Materials Science & Engineering Laboratory, National Institute for Standards and Technology, Gaithersburg, Maryland 20899; and NSLS, Brookhaven National Lab, Upton, New York 11973

Received December 16, 1999; Revised Manuscript Received July 28, 2000

ABSTRACT: Poly(styrene-*b*-semifluorinated isoprene) block copolymers with $-\text{CF}_2\text{H}$ -terminated side groups were synthesized by the esterification reaction of a poly(styrene-*b*-hydroxylated 1,2-/3,4-isoprene) block copolymer with semifluorinated acid chlorides. Two distinct first-order transitions were observed by DSC measurements in the resulting block copolymers at temperatures below the glass transition of polystyrene. The transition temperatures of the longer fluorocarbon units (10 $-\text{CF}_2-$ units) were found to be higher than the shorter fluorocarbon units (eight $-\text{CF}_2-$ units). By comparing the block copolymers having $-\text{CF}_3$ end groups with those with $-\text{CF}_2\text{H}$ end groups, it was found that both the thermal behavior and surface properties are significantly affected by the terminal group of the semifluorinated side chains in the block copolymer. NEXAFS spectroscopy reveals that, although the surface coverage by semifluorinated groups is roughly the same regardless of whether the ends are $-\text{CF}_2\text{H}$ or $-\text{CF}_3$, the orientational order of the $-\text{CF}_2\text{H}$ surfaces is significantly poorer than that of the $-\text{CF}_3$ surfaces. After long-term water exposure the $-\text{CF}_2\text{H}$ surfaces were observed to reconstruct to more hydrophilic ones even though the analogous polymers with $-\text{CF}_3$ -terminated semifluorinated side chains were quite stable. The ease of surface reconstruction is probably related to the relatively poor orientation order of the polymers with $-\text{CF}_2\text{H}$ end groups as determined by NEXAFS.

Introduction

Materials having low surface energy may be formed using fluorinated polymers such as poly(tetrafluoroethylene) (PTFE) and fluorinated ester side chain acrylic and methacrylic polymers or fluorinated block copolymers.^{1–6} It is well-known that some of the important factors in the behavior of low-energy surfaces include both the precise nature of the atoms populating a surface and their physical arrangement. Fluorinated polymers having $-\text{CF}_3$ end groups have been shown to have a lower surface energy than PTFE. However, in most fluorinated polymers, a potential problem in many applications has been the stability of these low-energy surfaces and their tendency to undergo surface reconstruction in a polar environments, e.g., in water. This issue has in most cases gone unresolved due to the poor stability of the amorphous fluorinated surface chains. Such materials cannot resist the movement of polar groups to their surface in an aqueous environment, thus limiting their practical application.

One possible strategy for creating stable, low surface energy materials uses the self-organizing character of liquid crystalline groups, such as those provided by semifluorinated segments.⁷ As reported in recent studies, it was also observed that self-organization in semifluorinated block copolymers was able to stabilize the surface against reconstruction after weeks of exposure to a polar liquid such as water.⁸ When the semifluorinated alkyl side chain contains more than eight $-\text{CF}_2-$ units and more than four $-\text{CH}_2-$ units, the resulting surfaces exhibited a low critical surface tension (ca. 8 mN/m) and a high water contact angle (ca. 120°/advancing, 110°/receding).⁷ We believe that these stable low-energy surfaces correspond to the smectic B phase.

To study the molecular nature of the polymer surface, studies using near edge X-ray absorption fine structure (NEXAFS) were carried out. This technique makes use of a polarized X-ray beam to probe molecular composition and orientation of the near surface region. From these studies, it was seen that the surface is made up of the fluorinated component to the extent that the other block (styrene) in these block copolymers is excluded from the surface region. At the same time, it was possible to demonstrate that the semifluorinated segments had a net orientation that was normal to the surface. The orientational order could be correlated with the architecture of the mesogen (i.e., number of $-\text{CF}_2-$ and $-\text{CH}_2-$ units).^{8,9} The orientational order for a given mesogen architecture decreases with increasing temperature through the smectic B (S_B) to smectic A (S_A)

[†] Cornell University.

[‡] Yamagata University.

[§] NCSU.

[‡] Department of Materials, UCSB.

[‡] Department of Chemical Engineering, UCSB.

[‡] National Institute for Standards and Technology.

[‡] Brookhaven National Lab.

[^] Present address: Corning Incorporated, Polymer Core Technology, Painted Post, NY 14870.

[‡] Present address: Uniroyal Chemical Company, Naugatuck, CT 06770.

to isotropic (I) transitions in the bulk polymer. Significant surface orientational order persisted, however, to temperatures well above the S_A to I bulk transition.¹⁰

Precise and stable control of surface organization is also a potentially useful feature of polar surfaces. To examine the possibility that semifluorinated groups in general might be capable of serving as structural templates for polar surfaces, a series of new polymers in which $-\text{CF}_2\text{H}$ end groups replace $-\text{CF}_3$ end groups were synthesized for the creation of new, controlled surface polymers. Our strategy was to exchange one hydrogen atom for a fluorine atom on the terminal perfluoromethyl segments, with the expectation of the remaining $-\text{CF}_2-$ helix still forming a closely packed surface. Since the $-\text{CF}_2\text{H}$ end groups are smaller than the $-\text{CF}_3$ end groups they replace, we do not expect this substitution to disrupt the packing on steric grounds. On the other hand, because of the increased dipolar character of the $-\text{CF}_2\text{H}$ function, the orientation order of the helices may be significantly reduced, thus calling into question the stability of these surfaces in a polar environment. In this regard the experiments of Mach et al.¹¹ on low molar mass liquid crystals (LMMLCs) comparing surface energies of LMMLCs with $-\text{CF}_2\text{H}$ end groups with those of LMMLCs with $-\text{CF}_3$ end groups suggest that this small replacement may have major consequences for polymer surface properties.

In this paper, we describe the synthesis and characterization of styrene-*b*-semifluorinated diene block copolymers containing $-\text{CF}_2\text{H}$ end groups. The surface character of these polymers was investigated by measurements of both contact angle and near edge X-ray absorption fine structure (NEXAFS). The $-\text{CF}_2\text{H}$ end groups produce a surface with lower water contact angles as well as poorer orientational order. These surfaces also reorganize to more hydrophilic surfaces upon prolonged exposure to water.

Experimental Section

Materials. 1*H*,1*H*,9*H*-Perfluoro-1-nanol (90%, Lancaster Synthesis Inc.), 1*H*,1*H*,11*H*-perfluoro-1-undecanol (Lancaster Synthesis Inc.), carbon tetraiodide (97%, Aldrich), 9-decen-1-ol (97%, Aldrich), tributyltin hydride (97%, Aldrich), nitrogen dioxide (99.5%, Aldrich), thionyl chloride (99%, Aldrich), pyridine (99.8%, Aldrich), α,α,α -trifluorotoluene (99%, Aldrich), and toluene (Fisher) were used as received. Triphenylphosphine (99%, Aldrich) was used after purification by recrystallization from *n*-hexane. 2,2'-Azobisisobutyronitrile (98%, Aldrich) was used after purification by recrystallization from acetone at 0 °C. 4-(Dimethylamino)pyridine (99%, Aldrich) was used after purification by recrystallization from benzene. THF (Fisher) was distilled from sodium benzophenone ketyl under nitrogen. Hydroxylated poly(styrene-*b*-isoprene) block copolymer was synthesized by reaction of hydroboration of poly(styrene-*b*-isoprene) block copolymer with 1,2- and 3,4-polyisoprene content greater than 97% which was synthesized by living anionic polymerization, as reported previously.⁹

Synthesis of Semifluorinated Acids. a. 1*H*,1*H*,9*H*-Perfluorononyl Iodide (1*a*). 1*H*,1*H*,9*H*-Perfluorononyl iodide (1*a*) was synthesized by iodination reaction of 1*H*,1*H*,9*H*-perfluoro-1-nanol with carbon tetraiodide.¹⁰ To a single-necked round-bottom 200 mL flask equipped with a condenser, a nitrogen inlet via septum rubber, and magnetic stirrer, the 1*H*,1*H*,9*H*-perfluoro-1-nanol (6.48 g, 15 mmol) and triphenylphosphine (7.86 g, 30 mmol) were dissolved in pyridine (15 mL) by stirring at room temperature. The solution was cooled to 0 °C, followed by the addition of carbon tetraiodide (7.79 g, 15 mmol) in several portions. The resulting mixture was stirred at this temperature for 1 h, and then the solution was gradually warmed and refluxed for 6 h. The color of the

solution turned from yellow to dark-brown. The end of the reaction was confirmed by using a TLC plate exposed to iodine vapor with *n*-hexane as the eluent solvent. After reaction, pyridine was removed by distillation under N_2 atmosphere. Diethyl ether was added to the residue, and the organic layer was successively washed with HCl(aq) (1 M), water, and saturated $\text{NaHCO}_3\text{(aq)}$. The organic layer was dried over anhydrous MgSO_4 , and the remaining solvents were evaporated under reduced pressure. The brown residue was purified twice by column chromatography with *n*-hexane as the eluent solvent to yield a white product. Yield 6.24 g (11.5 mmol, 77%). IR (NaCl): ν (cm^{-1}) = 3045, 2985, 2920, 2850 (C–H, st), 1420 (CH_2 , st), 1210, 1150 (C–F, st). ^1H NMR (200 MHz, CDCl_3): δ (ppm) = 3.64 (t, J = 17.1 Hz, CH_2 , 2H), 6.05 (tt, 2J = 51.9 Hz, 3J = 5.0 Hz $-\text{CF}_2\text{H}$, 1H).

b. 1*H*,1*H*,11*H*-Perfluoroundecyl Iodide (1*b*). Compound 1*b* was prepared by the reaction of 1*H*,1*H*,11*H*-perfluoro-1-undecanol with carbon tetraiodide. The procedure was the same as used for the synthesis of 1*a*. Yield 8.57 g (13.3 mmol, 89%). IR (NaCl): ν (cm^{-1}) = 3045, 2985, 2920, 2850 (C–H, st), 1420 (CH_2 , st), 1210, 1150 (C–F, st). ^1H NMR (200 MHz, CDCl_3): δ (ppm) = 3.63 (t, J = 17.1 Hz, CH_2 , 2H), 6.05 (tt, 2J = 51.9 Hz, 3J = 5.0 Hz $-\text{CF}_2\text{H}$, 1H).

c. 12,12,13,13,14,14,15,15,16,16,17,17,18,18,19,19,19*H*-Hexadecafluoro-1-nonadecanol (2*a*).^{7,11} To a three-necked round-bottom 200 mL flask equipped with a condenser, a nitrogen inlet via septum rubber, and magnetic stirrer, compound 1*a* (6.00 g, 11.0 mmol) and 9-decen-1-ol (2.96 mL, 16.5 mmol) were placed and heated to 80 °C. After the mixture was homogenized, 2,2'-azobisisobutyronitrile (27.5 mg, 0.167 mmol) was added and stirred at this temperature. After stirring for 12 h, the mixture was cooled to room temperature, and yellow, waxy solids were obtained. To the reaction mixture, 2,2'-azobisisobutyronitrile (0.180 g, 1.09 mmol) and tributyltin hydride (5.92 mL, 22.0 mmol) were added and dissolved in toluene (11 mL) under nitrogen at room temperature. The solution was heated to 80 °C and stirred for 24 h. After the reaction, toluene was removed by distillation under N_2 atmosphere. Flash column chromatography of the residue on silica gel with *n*-hexane removed the unreacted 2*a*, and the excess amount of 9-decen-1-ol and gave a white solid after the eluent solvent was changed to ethyl acetate. Furthermore, the product was purified by recrystallization from *n*-hexane three times. Yield 4.59 g (8.01 mmol, 73%). IR (NaCl): ν (cm^{-1}) = 3320 (O–H, st), 2925, 2855 (C–H, st), 1205, 1150 (C–F, st). ^1H NMR (200 MHz, CDCl_3): δ (ppm) = 1.15–1.46 (br, CH_2 and OH, 15H), 1.49–1.85 (br, CH_2 , 4H), 2.04 (tt, CH_2 , $J_{\text{H–H}}$ = 8.5 Hz, $J_{\text{H–F}}$ = 17.8 Hz, 2H), 3.64 (t, J = 6.4 Hz, CH_2 , 2H), 6.06 (tt, 2J = 52.0 Hz, 3J = 5.0 Hz $-\text{CF}_2\text{H}$, 1H).

d. 12,12,13,13,14,14,15,15,16,16,17,17,18,18,19,19,20,20,21,21*H*-Eicosafuoro-1-heneicosanol (2*b*). The procedure of compound 2*b* is the same as that used for the synthesis of 2*a*. Yield 5.32 g (7.92 mmol, 72%). IR (NaCl): ν (cm^{-1}) = 3335 (O–H, st), 2925, 2855 (C–H, st), 1210, 1150 (C–F, st). ^1H NMR (200 MHz, CDCl_3): δ (ppm) = 1.15–1.46 (br, CH_2 and OH, 15H), 1.49–1.85 (br, CH_2 , 4H), 2.04 (tt, CH_2 , $J_{\text{H–H}}$ = 8.5 Hz, $J_{\text{H–F}}$ = 17.8 Hz, 2H), 3.64 (t, J = 6.4 Hz, CH_2 , 2H), 6.06 (tt, 2J = 52.0 Hz, 3J = 5.0 Hz $-\text{CF}_2\text{H}$, 1H).

e. 12,12,13,13,14,14,15,15,16,16,17,17,18,18,19,19,19*H*-Hexadecafluoro-1-nonadecanoic acid (3*a*).^{7,12} Compound 2*a* (2.00 g, 3.5 mmol) was placed into a glass tube reactor (20 × 200 mm) equipped with a small magnetic stir bar and sealed with a Teflon stopcock. Nitrogen dioxide (1.61 g, 17.5 mmol) was introduced into the reactor at -78 °C, and the reactor was slowly warmed to room temperature. The reactor was dissolved in nitrogen dioxide and stirred for 1 h. The color of the compound turned from dark green to dark brown. The reactor was then slowly heated to 50 °C and held at this temperature for 48 h. After the reaction was cooled to room temperature, the stopcock was opened and excess nitrogen dioxide was removed. The white product was purified by sublimation under high vacuum. Yield 1.95 g (95%, 3.3 mmol). IR (NaCl): ν (cm^{-1}) = 3500–2500 (O–H, st), 2920, 2850 (C–H, st), 1700 (C=O, st), 1210, 1150 (C–F, st). ^1H NMR (200 MHz, CDCl_3): δ (ppm) = 1.15–1.85 (br, CH_2 , 16H), 2.03 (tt,

CH₂, $J_{\text{H-H}} = 8.5$ Hz, $J_{\text{H-F}} = 17.8$ Hz, 2H), 2.38 (t, $J = 7.3$ Hz, CH₂, 2H), 6.06 (tt, $^2J = 52.0$ Hz, $^3J = 5.0$ Hz -CF₂H, 1H), 6.92–8.45 (br, COOH, 1H).

f. 12,12,13,13,14,14,15,15,16,16,17,17,18,18,19,19,20,20,21,21,21H-Eicosafuoro-1-heneicosanoic acid (3b). The procedure of compound **3b** is the same as that used for the synthesis of **3a**. Yield 1.83 g (76%, 2.66 mmol). IR (NaCl): ν (cm⁻¹) = 3500–2500 (O–H, st), 2920, 2850 (C–H, st), 1700 (C=O, st), 1210, 1150 (C–F, st). ¹H NMR (200 MHz, CDCl₃): δ (ppm) = 1.15–1.85 (br, CH₂, 16H), 2.03 (tt, CH₂, $J_{\text{H-H}} = 8.5$ Hz, $J_{\text{H-F}} = 17.8$ Hz, 2H), 2.38 (t, $J = 7.3$ Hz, CH₂, 2H), 6.06 (tt, $^2J = 52.0$ Hz, $^3J = 5.0$ Hz -CF₂H, 1H), 8.31–8.69 (br, COOH, 1H).

g. 12,12,13,13,14,14,15,15,16,16,17,17,18,18,19,19,19H-Hexadecafluoro-1-nonadecanoic Acid Chloride (4a). The semifluorinated acid chloride **4a** was prepared by reaction of **3a** with thionyl chloride. To a single-necked round-bottom 10 mL flask equipped with a nitrogen inlet via septum rubber and magnetic stirrer, **3a** (1.50 g, 2.55 mmol) and thionyl chloride (0.5 mL) were added at 0 °C. The solution was slowly heated to 40 °C and stirred for 2 h at this temperature. After the reaction, the excess amount of thionyl chloride was removed using a vacuum aspirator. The crude product was purified by distillation under high reduced pressure to give **4a**. Yield 1.37 g (89%, 2.26 mmol). IR (NaCl): ν (cm⁻¹) = 2935, 2860 (C–H, st), 1800 (C=O, st), 1210, 1150 (C–F, st).

h. 12,12,13,13,14,14,15,15,16,16,17,17,18,18,19,19,20,20,21,21,21H-Eicosafuoro-1-heneicosanoic Acid Chloride (4b). The procedure of compound **4b** is the same as that used for the synthesis of **4a**. Yield 1.17 g (75%, 1.66 mmol). IR (NaCl): ν (cm⁻¹) = 2930, 2860 (C–H, st), 1800 (C=O, st), 1210, 1150 (C–F, st).

Attachment Reaction (5a).⁷ Attachment reaction of compound **4a** with the hydroxylated block copolymer was carried out in a dry 10 mL flask, in which 300 mg of the hydroxylated block copolymer (0.632 mmol of OH group) and a catalytic amount of 4-(dimethylamino)pyridine (3.6 mg, 0.03 mmol) were dissolved in 2 mL of distilled THF and 0.5 mL of pyridine. After the hydroxylated block copolymer was completely dissolved in the cosolvent, a 10 wt % THF solution of **4a** (0.483 g, 0.80 mmol) was injected slowly into the reaction flask through a rubber septum at room temperature. The reaction solution was slowly heated to 45 °C and stirred for 24 h at this temperature. After the reaction, the polymer solution was poured into a large amount of solvent mixture of methanol/water 1:1 (v/v). The product was collected and washed with methanol/water. The obtained product was dissolved in THF, and then the solution was poured into methanol/water 1/1 (v/v) five times and into methanol twice to remove excess **4a** and pyridine salt. Polymer **5a** was collected, washed with methanol, and dried in vacuo at 50 °C for 24 h. Yield 0.624 g (93%). IR (NaCl): ν (cm⁻¹) = 3060, 3025, 2925, 2855 (C–H, st), 1735 (C=O, st), 1600, 1490 (benzene ring, st), 1450 (C–O–C, st), 1210, 1150 (C–F, st).

The procedure of **5b** is the same as that used for the synthesis of **5a**. Yield 0.662 g (90%). IR (NaCl): ν (cm⁻¹) = 3060, 3025, 2925, 2855 (C–H, st), 1735 (C=O, st), 1600, 1490 (benzene ring, st), 1450 (C–O–C, st), 1215, 1155 (C–F, st).

Characterization. Infrared spectra were measured with a Mattson 2020 Galaxy series Fourier transform infrared spectrometer with 4 cm⁻¹ resolution using 64 scans. Samples were pressed in a KBr tablet or cast on a NaCl crystal plate.

Proton NMR spectra were obtained on a Varian 200 spectrometer at ¹H, 200 MHz. Deuterated chloroform was used as the solvent.

Gel permeation chromatography (GPC) was carried out using four Waters Styragel HT columns operating at 31 °C. The effective molecular weight range of the columns is from 500 to 10⁷. GPC data were collected using a Waters 490 programmable multiwavelength detector. Molecular weights are quoted with respect to monodisperse polystyrene standards. THF was used as solvent and the GPC operated at 0.3 mL/min. Block copolymers were dissolved in THF at a concentration of 3.0 mg/mL. Polymer solution volumes of 20 μ L were used for GPC measurements.

Thermogravimetric analysis (TGA) measurement was performed on a Perkin-Elmer TGA-7 series instrument. Samples of ca. 5 mg were analyzed using a 10 °C/min heating and cooling rate. Nitrogen was used as purge gas at the flow rate of 40 mL/min.

Differential scanning calorimeter (DSC) measurement was performed on a Perkin-Elmer DSC-7 series instrument. Samples of ca. 10 mg were analyzed using a 10 °C/min heating and cooling rate. Nitrogen was used as purge gas at a flow rate of 40 mL/min.

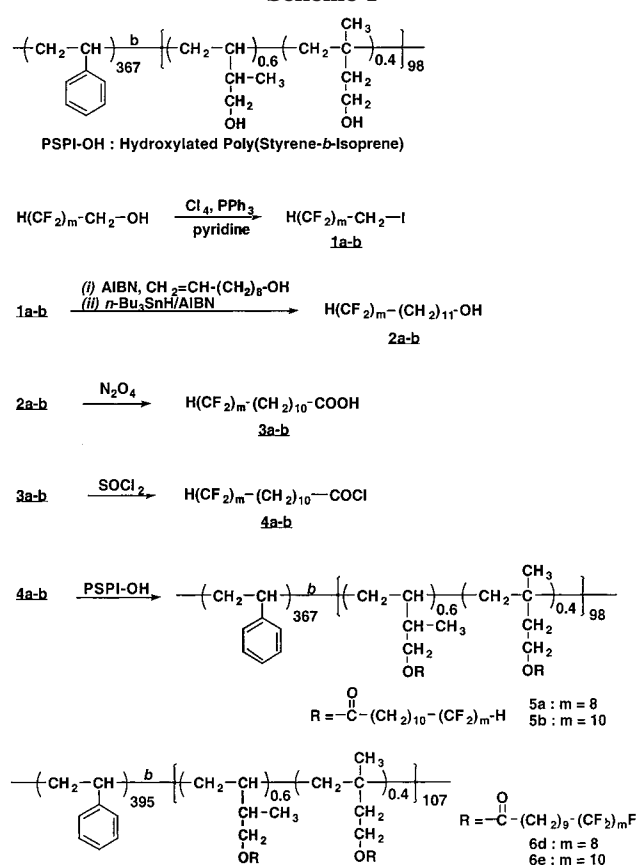
Contact angles were determined using a NRL contact angle goniometer model 100-00 (Ramé-Hart Inc.) at 20 °C. Films were prepared by spin coating a 5 wt % block copolymer/ α,α,α -trifluorotoluene solution on a silicon wafer at room temperature. The contact angles were averaged over five measurements. The advancing contact angle was read by injecting 4 μ L liquid drops. The receding contact angles were measured by removing 3 μ L of liquid from the droplet while the static contact angle was obtained using a free drop of liquid (ca. 4 μ L) on the film surface.

Our NEXAFS experiments measure the resonant soft X-ray excitation of a carbon 1s electron to a σ^* orbital, an unoccupied low-lying antibonding molecular orbital with σ symmetry.¹⁵ The NEXAFS experiments were carried out on the NIST/Dow materials characterization end station on the U7A beamline at the National Synchrotron Light Source at Brookhaven National Laboratory. This beamline is equipped with a toroidal mirror spherical grating monochromator. The incident photon energy resolution and intensity were 0.2 eV and 5×10^{10} photons/s, respectively, for an incident photon energy of 300 eV and a typical storage ring current of 500 mA. The X-rays are elliptically polarized, with the electric field vector **E** dominantly in the plane of the storage ring (polarization factor = 0.85). Polymer films approximately 200 nm thick were prepared by spin-casting onto silicon wafers from trifluorotoluene solutions and annealed for 6 h in a vacuum at 150 °C. Each polymer sample was mounted on a stage positioned by a goniometer that allows the angle of the sample surface with regard to the polarization vector of the soft X-rays to be varied between 20° and 90°. Since the 1s $\rightarrow \sigma^*$ resonant excitations are governed by dipole selection rules, the transitions are polarized; i.e., their intensity varies as a function of the direction of the electric field vector **E** of the incident X-ray photon relative of the long axis of the σ^* orbital of the final state. In our experiments we detect the resonant excitation by monitoring the emission of Auger electrons from the near surface region of the polymer film. These Auger electrons form most of the partial electron yield (PEY) signal that is collected using a channeltron electron multiplier that has an adjustable entrance grid bias (EGB). Auger electrons that have lost significant energy in emerging from more than 2 nm below the surface are discriminated against by increasing the negative EGB on the channeltron detector. The monochromator energy and resolution were calibrated by comparing the transmission spectrum from gas-phase carbon monoxide with electron energy loss reference data. To eliminate the effect of incident beam intensity fluctuations and monochromator absorption features, the PEY signal was normalized by the incident beam intensity obtained from the photoyield of a clean gold grid.

Results and Discussion

Synthesis. The base poly(styrene-*b*-isoprene) block copolymer was prepared by anionic polymerization to form styrene and isoprene blocks with degrees of polymerization of 367 and 98, respectively. The polyisoprene block had 60% 1,2- and 40% 3,4- units as characterized by ¹H NMR spectrum. This base polymer was nearly identical in structure and composition to the semifluorinated block copolymers with -CF₃ end groups described in a previous report (styrene/395, isoprene/107).⁷ The base block copolymer was modified using quantitative hydroboration chemistry, retaining its nar-

Scheme 1



row molecular weight distribution after hydroxylation according to GPC measurements. A synthetic procedure for the preparation of the modified block copolymers prepared for this study is illustrated in Scheme 1. We selected fluorocarbon chain lengths of eight and 10 $-\text{CF}_2-$ units for comparison to the polymers with $-\text{CF}_3$ end groups described previously. However, it should be noted that the hydrocarbon segments were one $-\text{CH}_2-$ unit longer than the prior semifluorinated block copolymers because the appropriate starting materials were not commercially available. The attachment reaction of the semifluorinated side groups to the hydroxylated poly(styrene-*b*-isoprene) block copolymer was carried out by reaction with the semifluorinated acid chloride. The yield of the attachment esterification was nearly quantitative as seen from FTIR and ^1H NMR measurements. The FTIR spectra showed no residual $-\text{OH}$ groups and also the strong absorbance of the carbonyl peak at 1735 cm^{-1} derived from the ester linkage after the esterification reaction. In the ^1H NMR spectra, the proton signals of the terminal $-\text{CF}_2\text{H}$ groups appeared around 6.05 ppm as a result of the inter- and intramolecular coupling with adjacent fluorine atoms (Figure 1). These findings clearly indicate the formation of the expected block copolymers.

GPC Measurements of the Semifluorinated Block Copolymers with $-\text{CF}_2\text{H}$ End Group. The molecular weights by GPC measurements of the poly(styrene-*b*-hydroxylated isoprene) block copolymer and the semifluorinated block copolymers with $-\text{CF}_2\text{H}$ end groups **5a** and **5b** are reported in Table 1, and their GPC plots of UV absorption versus elution time are shown in Figure 2. The number-average molecular weight of the polystyrene block of the starting poly(styrene-*b*-isoprene) block copolymer was found to be 38 200 by GPC.

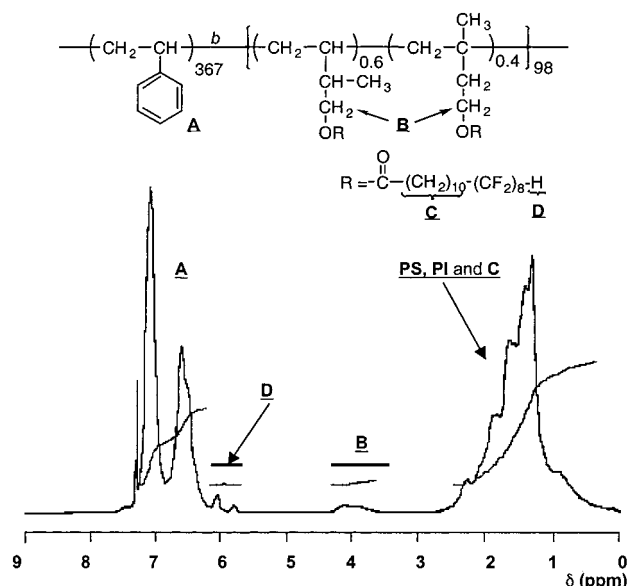


Figure 1. ^1H NMR spectra of poly(styrene-*b*-semifluorinated isoprene) block copolymers with $-\text{CF}_2\text{H}$ end groups **5a** in CDCl_3 .

Table 1. GPC Data of Poly(styrene-*b*-semifluorinated isoprene) Block Copolymers with $-\text{CF}_2\text{H}$ End Groups^a

polymer	calcd M_n ratio of PS/semifluorinated block	M_n	M_w	M_w/M_n
PS/hydroxylated PI		44.9K	46.3K	1.03
5a	38.2K/64.1K	67.8K	87.4K	1.29
5b	38.2K/73.9K	63.9K	76.7K	1.20

^a Polystyrene was used as standard for calculating molecular weight.

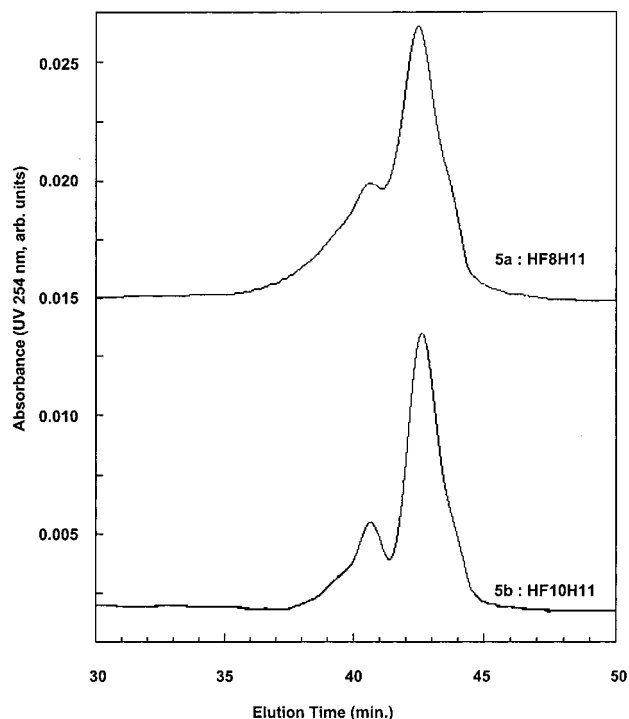


Figure 2. Gel permeation chromatograms of poly(styrene-*b*-semifluorinated isoprene) block copolymers with $-\text{CF}_2\text{H}$ end groups.

The ^1H NMR results allowed calculation of the styrene/isoprene molar ratio and hence showed the polyisoprene block molecular weight to be 6700. The semifluorinated

Table 2. Thermal Data of Poly(styrene-*b*-semifluorinated isoprene) Block Copolymers

polymer	side chain ^a (end group)	<i>T</i> _g of PS (°C)	<i>T</i> _A (°C)	<i>T</i> _B (°C)	ΔH_{m1} ^b (J/g)	ΔH_{m2} ^b (J/g)
5a	HF8H11 (–CF ₂ H)	101	42.7		0.01	3.80
6d ^c	F8H10 (–CF ₃)	101	49.9	72.2	10.3	0.94
5b	HF10H11 (–CF ₂ H)	102	52.1	74.1	0.64	3.89
6e ^c	F10H10 (–CF ₃)	102	97.1	114.4	11.5	0.78

^a Semifluorinated 1-alcohol (see Scheme 1). ^b Calculated as per gram semifluorinated side chain. ^c Reference 7.

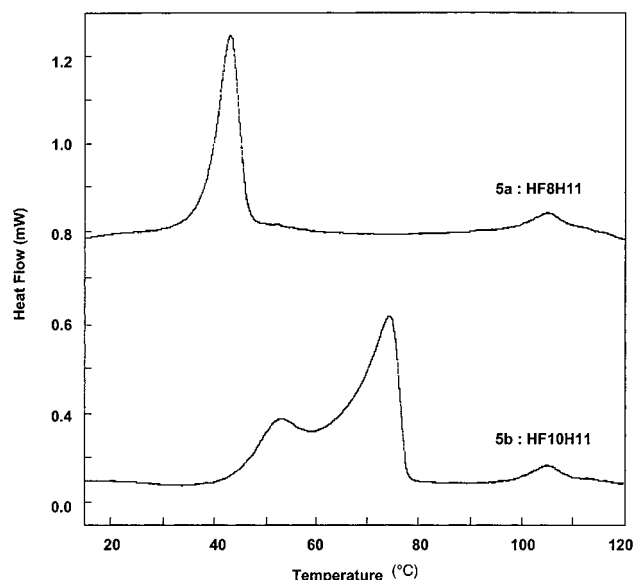


Figure 3. Differential scanning calorimetry (DSC) scans of poly(styrene-*b*-semifluorinated isoprene) block copolymers with –CF₂H end groups (heating rate 10 °C/min).

block copolymers with –CF₂H end groups **5a** and **5b** showed bimodal peaks in their GPC chromatograms. The higher molecular weight peaks are due to the micellar aggregation of the semifluorinated block copolymers in the THF solution, since such block copolymers have been found previously to form micelles in this solvent.⁷

Thermal Properties. The thermal behavior of the semifluorinated block copolymers with –CF₂H end groups **5a** and **5b** was examined by thermogravimetric analysis (TGA) and differential scanning calorimetry (DSC). These polymers were found to be stable to ~270 °C. The results of DSC measurements of the semifluorinated block copolymers with –CF₂H end groups **5a** and **5b** are listed in Table 2, and the DSC traces are shown in Figure 3. To eliminate the effect of thermal history on sample transitions, all the samples were heated to 160 °C and held for 1 min at this temperature before cooling to –65 °C at a rate of 10 °C/min. All DSC data reported were obtained from the second run.

As illustrated in Table 2, a first-order transition was observed at temperature *T*_A for both polymers **5a** and **5b** below the glass transition of polystyrene, but only polymer **5b** showed a second, low-temperature, transition, *T*_B. The transitions at temperatures *T*_B and *T*_A of **5b** are ~12 and ~30 °C higher, respectively, than the single transition (*T*_A) of **5a** which occurs at 43 °C. The differences in thermal behavior between the semifluorinated block copolymers with –CF₂H (**5a** and **5b**) and –CF₃ (**6d** and **6e**) end groups can be summarized as follows: the transition temperatures *T*_A of **5a** and **5b** are lower than those of **6d** and **6e**. The transition enthalpy ΔH_A of both **5a** and **5b** are similar but larger than the *S*_A to *I* transition in **6d** and **6e**. On the other

Table 3. Surface Properties of Poly(styrene-*b*-semifluorinated isoprene) Block Copolymers

polymer	side chain ^a (end group)	H ₂ O contact angle (deg)		crit surf. tension (mN/m)
		advancing	receding	
5a	HF8H11 (–CF ₂ H)	101	89	20.5
6d ^b	F8H10 (–CF ₃)	122	110	8.2
5b	HF10H11 (–CF ₂ H)	102	89	16.5
6e ^b	F10H10 (–CF ₃)	123	112	8.0

^a Semifluorinated 1-alcohol. ^b Reference 7.

hand, the enthalpy ΔH_B of polymer **5b** is smaller than that of the *S*_B to *S*_A transition of either **6d** or **6e**. However, the total enthalpy $\Delta H_{total} = \Delta H_A + \Delta H_B$ of LC disordering from room temperature to the isotropic state of the –CF₃ (**6d** and **6e**) polymers is larger than that of the –CF₂H (**5a** and **5b**) polymers. The room-temperature X-ray diffraction patterns of these –CF₂H-terminated semifluorinated block copolymers are consistent with a smectic A mesophase (**5a** has a spacing of ~39 Å and **5b** has a spacing of ~50 Å). Like the –CF₃ series, this is consistent with a smectic arrangement having a bilayer structure. The small thermal transition observed in polymer **5b** at 52 °C can be explained as a *S*_B to *S*_A transition for a minor fraction of the polymer. The X-ray and the thermal measurements, especially a comparison of the total enthalpy of LC disordering, suggest that the semifluorinated block copolymers with –CF₃ end groups form more ordered and stable mesophases at room temperature than those block copolymers with –CF₂H end groups.

Hydrophobic Properties of Semifluorinated Side Chain Block Copolymers. To obtain an indication of the hydrophobicity of the surface, water contact angle measurements were performed, and the results are listed in Table 3. The advancing water contact angles of **5a** and **5b** (102°) are about 20° lower than those of the –CF₃-terminated block copolymers (**6d** and **6e**) and also are about 6° lower than the values reported for poly(tetrafluoroethylene) (PTFE) (advancing/108°, receding/88°).¹³

The critical surface tension of these polymers is also reported in Table 3. The critical surface tension was determined from the advancing contact angles θ of a homologous series of linear alkanes and two low molecular weight trimethylsilyl-terminated poly(dimethylsiloxane)s with known surface tension γ . A Zisman plot of $\cos \theta$ versus γ was extrapolated to $\cos \theta = 1$ to find the critical surface tension, which is taken as a measure of the surface tension of the film. While the critical surface tensions of **6d** and **6e** are very low, 8.2 and 8.0 mN/m, respectively, consistent with these films having an all –CF₃ surface, the substitution of a single H for an F on the end group produces large increases in the critical surface tension. Moreover **5a**, with the shorter –CF₂– helix, has a considerably higher critical surface tension (20.5 mN/m) than **5b**, which has a longer –CF₂– helix (16.5 mN/m). Clearly the critical surface

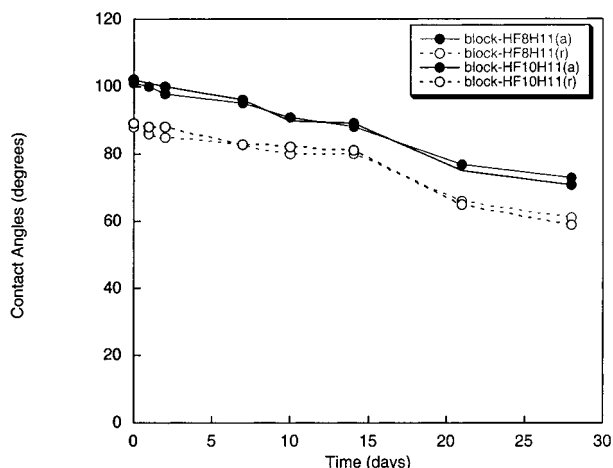


Figure 4. Time-dependent advancing (a) and receding (r) water contact angles measured on films of samples **5a** and **5b**, $-\text{CF}_2\text{H}$ -terminated semifluorinated side chain polymers.

tension is quite sensitive to the changes in end group chemistry, a conclusion that is entirely consistent with the direct measurements of Mach et al.¹¹ of the surface tensions of low molar mass liquid crystals with partly fluorinated end groups.

To investigate the surface stability of the films, long-term contact angle measurements were carried out by immersion of the films in water for 4 weeks at 22 °C (Figure 4). Both the advancing and receding water contact angles of **5a** and **5b** gradually decreased with time and dropped after 2 weeks to about 90° and 80°, respectively. The water contact angles continued to decrease to 70° and 60°, respectively, after 4 weeks to values that are about 40° lower than those of the original films. On the other hand, the water contact angles of **6d** and **6e** exhibited no change after 2 weeks of immersion in water. Previously, the water contact angles of polymers with ~ 6 $-\text{CF}_2-$ units in the semifluorinated side group were shown to drop to about 40° lower than that of the original unimmersed films. This behavior has been ascribed to the presence of a room-temperature smectic A phase that has a much lower order mesophase than the smectic B phase found in the polymer with $-\text{CF}_3$ end groups.⁷ The surface can reconstruct to expose the more polar ester groups by reorientation of several semifluorinated groups without paying a relatively high enthalpy penalty. Thus, one reason for the differences between the observed surface stability of the $-\text{CF}_2\text{H}$ and $-\text{CF}_3$ end groups is due to the weaker barrier to surface reconstruction provided by the smectic A phase when in contact with water.

The unreconstructed surfaces of **5a** and **5b** ($-\text{CF}_2\text{H}$ end groups) are less hydrophobic than those of **6d** and **6e** ($-\text{CF}_3$ end groups) or even PTFE ($-\text{CF}_2-$ groups). This decreased hydrophobicity is possibly due to the increased polarity of the end group by the introduction of a hydrogen atom. Calculated values of dipole moment for perfluorohexane were 0 D while simple replacement of the terminal F with H resulted in a calculated dipole moment of 1.7 D. These simple calculations made using molecular modeling¹⁴ show there is a significant increase in polarity due to the new structure of the semifluorinated side group. To assess whether the change in surface properties were due to this molecular level change or were due to major structural changes, the surface properties of these films were further evaluated using NEXAFS.

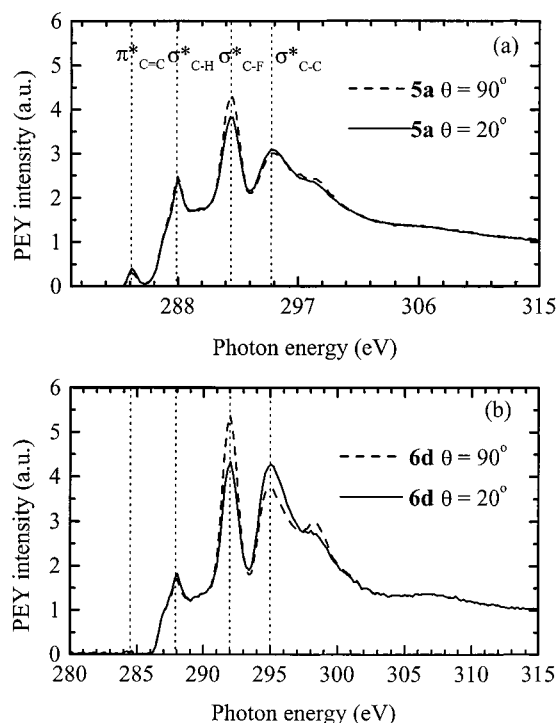


Figure 5. NEXAFS partial electron yield intensity versus X-ray photon energy for angles θ between the electric field vector of the polarized X-rays and the sample normal of 90 and 20°: (a) sample **5a** ($-\text{CF}_2\text{H}$ end groups); (b) sample **6d** ($-\text{CF}_3$ end groups).

Near Edge X-ray Absorption Fine Structure Experiments. Figure 5a shows the partial electron yield (PEY) signal as a function of soft X-ray photon energy over the region of the C K-edge for **5a** while Figure 5b shows similar data for **6d**. Two curves are shown on each plot: one corresponding to an angle θ between the electric field vector \mathbf{E} of the polarized X-ray beam and the surface normal of 90° and one corresponding to an angle θ of 20°. Similarly Figure 6a shows the PEY signal as a function of soft X-ray photon energy for **5b** while Figure 6b shows similar data for **6e**. Note that there is only a small PEY signal from the $1s \rightarrow \pi^*$ transition ($E = 284.5$ eV) of the phenyl rings of the polystyrene (PS) block in any of these plots even though the corresponding resonance is the strongest feature of the X-ray fluorescence yield spectrum of each of these samples. The absence of this resonance in the PEY spectrum means that there is almost no PS within 2 nm of the surface of any of these samples; i.e., the sample surfaces consist almost exclusively of the semifluorinated isoprene block.

Also marked on each plot are the resonant energies of the $1s \rightarrow \sigma^*$ transitions for the C-H ($E = 287.9$ eV), C-F ($E = 292.0$ eV), and C-C ($E = 295.0$ eV) bonds. In all cases the C-F $1s \rightarrow \sigma^*$ PEY signal is larger at $\theta = 90^\circ$ than at $\theta = 20^\circ$ while the C-C $1s \rightarrow \sigma^*$ PEY signal is larger at $\theta = 20^\circ$ than at $\theta = 90^\circ$. The PEY spectra, which were measured at the intermediate angles of $\theta = 30, 40, 55, 60, 70$, and 80° lie between the 90° and 20° extremes, but are not shown in Figures 5 and 6 for clarity. The spectra show that in all samples there is some orientational order of the C-F and C-C bonds near the surface. The fact that the C-F $1s \rightarrow \sigma^*$ PEY signal is larger at $\theta = 90^\circ$ than at $\theta = 20^\circ$ means that the C-F bonds are at least somewhat oriented parallel to the sample surface whereas the anisotropy in the C-C $1s \rightarrow \sigma^*$

Table 4. Surface Orientational Order Parameters and Average Helix Angles

sample	S_{CF} (C–F σ bond)	S_{CC} (C–C σ bond)	S_{helix} –CF ₂ – helix	$\langle\tau_{F-helix}\rangle$ (deg)
5a (–CF ₂ H end groups)	-0.059 ± 0.014	0.037 ± 0.010	0.118 ± 0.028	50.1 ± 1.1
6d (–CF ₃ end groups)	-0.120 ± 0.021	0.090 ± 0.011	0.240 ± 0.042	45.4 ± 1.6
5b (–CF ₂ H end groups)	-0.113 ± 0.013	0.150 ± 0.010	0.226 ± 0.026	45.9 ± 1.0
6e (–CF ₃ end groups)	-0.143 ± 0.015	0.130 ± 0.011	0.286 ± 0.030	43.6 ± 1.2

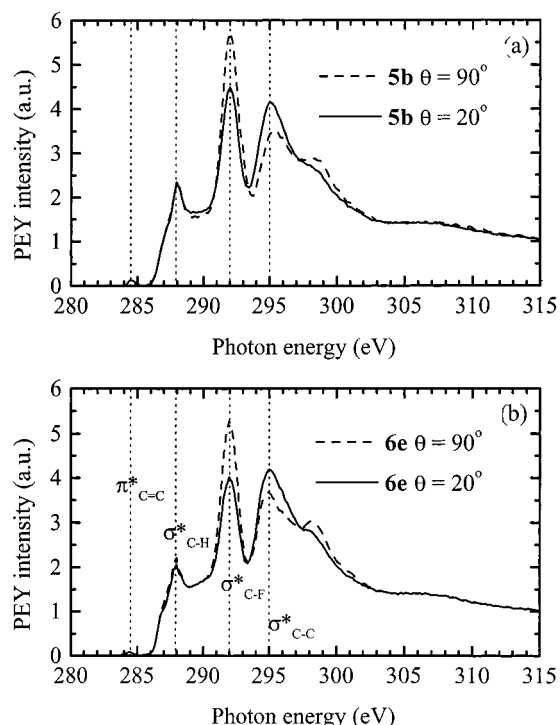


Figure 6. NEXAFS partial electron yield intensity versus X-ray photon energy for angles θ between the electric field vector of the polarized X-rays and the sample normal of 90 and 20°: (a) sample **5b** (–CF₂H end groups); (b) sample **6e** (–CF₃ end groups).

PEY signal means that these bonds have some net orientation normal to the sample surface. These results are consistent with previous ones on the semifluorinated LC block copolymers^{8,9} and indicate that the rigid –CF₂– helix is, on the average, oriented close to the sample normal to the sample surface. The degree of that orientation or the orientational order, however, is clearly different for the different samples. The surfaces of samples with –CF₂H end groups, **5a** and **5b**, are clearly much less oriented than their counterparts with –CF₃ end groups, **6d** and **6e**. In addition, the surfaces of the samples (**5b** and **6e**) with longer –(CF₂)– sequences are more highly ordered than those (**5a** and **6d**) with the shorter –(CF₂)– sequences.

To quantify the orientational order, we first follow the method of Outka and co-workers¹⁶ and fit the PEY NEXAFS spectra to a series of Gaussian curves representing the different $1s \rightarrow \sigma^*$ transitions and a step function corresponding to the excitation edge of carbon. We designate the magnitude of these Gaussians as the intensities $I(\theta)$ of the various $1s \rightarrow \sigma^*$ transitions. Adopting the notation of Stöhr and Samant,¹⁷ we define molecular orientation factors f_x , f_y , and f_z for the C–F and C–C bonds as follows:

$$f_z = \int \cos^2 \alpha f(\alpha) d\Omega$$

$$f_x = f_y = \frac{1 - f_z}{2}$$

where z is an axis normal to the film surface and x and y are orthogonal axes in the plane of the surface while α is the angle between the axis of the σ^* orbital (σ bond axis) and z . The molecular axis distribution function $f(\alpha)$ is normalized so that $\int f(\alpha) d\Omega = 1$ and thus $f_x + f_y + f_z = 1$. A uniaxial orientation order parameter S can then be defined as

$$S = \frac{1}{2}(3f_z - 1) \quad (1)$$

where S ranges from +1 (σ bond axis completely aligned along z) to $-1/2$ (σ bond axis lying in the plane of the surface). In the above treatment we assume that there is fiber symmetry normal the plane of the surface; i.e., there is no preferred direction in the plane, an assumption that must hold for our samples. The order parameter defined in this way is analogous to the Hermans orientation parameter of X-ray diffraction.¹⁸

Regardless of the amount of orientation of the σ bond normal to the plane, the PEY intensity $I(\theta)$ is predicted to have the following form:

$$I(\theta) = A + B \sin^2 \theta \quad (2)$$

The orientational order parameter S can be determined from the values of A and B ¹⁷ as follows:

$$S = -\frac{P^{-1}B}{3A + (3 - P^{-1})B} \quad (3)$$

where P is the polarization factor of the X-ray beam (0.85 in our case).

We have fit the C–F and C–C PEY $I(\theta)$ data for **5a**, **5b**, **6d**, and **6e** to eq 2 and then used eq 3 to extract values of S for these bonds. These results are displayed in Table 4.

Previously we used detailed calculations based on the “building block model”^{15,16} to determine the average tilt angle $\langle\tau_{F-helix}\rangle$ of the fluorocarbon helix part of single semifluorinated groups with respect to the surface normal.⁸ This average tilt angle can be shown to be directly related to the CF orientational order parameter S_{CF} as follows:

$$S_{CF} = \frac{1}{2} \left(\frac{3}{2} \sin^2 \langle\tau_{F-helix}\rangle - 1 \right) \quad (4)$$

Equation 4 can be inverted to yield $\langle\tau_{F-helix}\rangle$ values from values of S_{CF} and values of $\langle\tau_{F-helix}\rangle$ determined in this way are also given in Table 4. It is straightforward to define the order parameter S_{helix} of the –CF₂– helix axis relative the surface normal, viz.

$$S_{helix} \equiv -2S_{CF}$$

The values of S_{helix} are included in Table 4.

As can be seen in Table 4, while the longer **5b** shows much more surface orientational order than the shorter **5a**, in keeping with its lower critical surface tension (16.5 versus 20.5 mN/m), both semifluorinated block copolymers with –CF₂H end groups show less surface

orientational order than their counterparts with $-\text{CF}_3$ end groups, which also have much lower critical surface tensions (8.2 mN/m for **6d** and 8.0 mN/m for **6e**⁷). This increased disorder probably plays a role in the decreased hydrophobic character of their surfaces when compared to those of **6d** and **6e**, although the major part of the decrease in water contact angle and increase in critical surface tension probably arises from the dipolar nature of the $-\text{CF}_2\text{H}$ end groups themselves. More importantly, however, it seems likely that the less ordered surfaces of **5a** and **5b** will more easily reconstruct in water, and this is in fact the case. While the surfaces of **6e** and **6d** show advancing and receding contact angles that are stable for periods up to 2 weeks in water, those of **5a** and **5b** show dramatic declines over the same time period, decreasing up to 15° . In any case, it is clear that NEXAFS spectroscopy offers a very powerful method to characterize the orientational order of the fluorocarbon polymer surfaces.

Conclusions

In this paper, studies of the effect of single atom changes on surface behavior were carried out using block copolymers with surface active semifluorinated groups terminated with a $-\text{CF}_2\text{H}$ function. A substantial decrease in water contact angle and contact angle stability after prolonged water exposure was observed in comparison to analogous polymers prepared with $-\text{CF}_3$ terminal groups. NEXAFS studies show that these surfaces consisted only of the fluorinated block and that the styrene block is buried more than 2 nm below the surface. Orientational order parameters from NEXAFS showed that while the $-\text{CF}_2-$ helix of the polymer with $-\text{CF}_2\text{H}$ end groups has a net orientation normal to the surface, the helix of this surface was not as highly oriented as that of the analogous polymer with $-\text{CF}_3$ terminal groups; X-ray and thermal measurements show that the block copolymers with $-\text{CF}_3$ end groups form more stable and ordered mesophases than those of with $-\text{CF}_2\text{H}$ end groups. Both the room-temperature orientation and stability of the surface seems to be influenced by the lower stability of the smectic phase of the $-\text{CF}_2\text{H}$ -terminated polymers relative to that of the $-\text{CF}_3$ -terminated polymers. Thus, we believe that the increase in surface polarity is largely due to the change from a terminal $-\text{CF}_3$ group to a $-\text{CF}_2\text{H}$ function while the presence of the lower stability smectic mesophase is largely responsible for the decreased surface stability.

Acknowledgment. This research was supported by the Office of Naval Research, Grant N00014-95-1-0695.

Partial support from the NSF, Division of Materials Research, Polymers Program, under Grants DMR98-03738, DMR-9972863 and DMR93-214573 is also appreciated. The work at NCSU was supported by start-up funds from NCSU and from a NSF Career Award to J.G. The experimental assistance of Sharadha Sambasivan, Dr. Robert Bubeck, and Yushi Ando is gratefully acknowledged. T.H. thanks Narayan Sundararajan and Padma Gopalan for their kind help and many useful discussions. NEXAFS experiments were carried out at the National Synchrotron Light Source, Brookhaven National Laboratory, which is supported by the U.S. Department of Energy, Division of Materials Sciences and Division of Chemical Sciences.

References and Notes

- (1) Burnett, M. K.; Zisman, W. A. *J. Phys. Chem.* **1960**, *64*, 1292.
- (2) Schmidt, D. L.; Coburn, C. E.; Dekoven, B. M.; Potter, G. E.; Meyers, G. F.; Fisher, D. A. *Nature* **1994**, *368*, 39.
- (3) Hwang, S. S.; Ober, C. K.; Perutz, S. M.; Iyengar, D. R.; Schneggenburger, L. A.; Kramer, E. J. *Polymer* **1995**, *36*, 1321.
- (4) Iyengar, D. R.; Perutz, S. M.; Dai, C.-A.; Ober, C. K.; Kramer, E. J. *Macromolecules* **1996**, *29*, 1229.
- (5) Chapman, T. M.; Benrashed, R.; Marra, K. G.; Keener, J. P. *Macromolecules* **1995**, *28*, 331.
- (6) Chapman, T. M.; Marra, K. G. *Macromolecules* **1995**, *28*, 2081.
- (7) Wang, J.; Mao, G.-P.; Ober, C. K.; Kramer, E. J. *Macromolecules* **1997**, *30*, 1906.
- (8) Genzer, J.; Sivaniah, E.; Kramer, E. J.; Wang, J.; Körner, H.; Xiang, M.; Char, K.; Ober, C. K.; DeKoven, B. M.; Bubeck, R. A.; Chaudhury, M. K.; D. A.; Fischer, D. A. *Macromolecules* **2000**, *33*, 1882.
- (9) Genzer, J.; Sivaniah, E.; Kramer, E. J.; Wang, J.; Körner, H.; Char, K.; Ober, C. K.; DeKoven, B. M.; Bubeck, R. A.; Fischer, D. A.; Sambasivan, S. *Langmuir* **2000**, *16*, 1993.
- (10) Muthukumar, M.; Ober, C. K.; Thomas, E. L. *Science* **1997**, *277*, 1225.
- (11) Mach, P.; Huang, C. C.; Strobe, T.; Wedell, E. D.; Nguyen, T.; de Jeu, W. H.; Guittard, F.; Naciri, J.; Shashidhar, R.; Clark, N.; Jiang, I. M.; Kao, F. J.; Liu, H.; Nohira, H. *Langmuir* **1998**, *14*, 4330.
- (12) Mao, G.-P.; Wang, J.; Clingman, S. R.; Ober, C. K.; Chen, J. T.; Thomas, E. L. *Macromolecules* **1997**, *30*, 2556.
- (13) Anisuzzaman, A. K. M.; Whistler, R. L. *Carbohydr. Res.* **1978**, *61*, 511.
- (14) Molecular modelling was carried out using MacSpartan (WaveFunction, Inc.) with the AM1 semiempirical model.
- (15) Stöhr, J. *NEXAFS Spectroscopy*; Springer-Verlag: Berlin, 1992.
- (16) Outka, D.; Stöhr, J.; Rabe, J.; Swalen, J. D. *J. Chem. Phys.* **1988**, *88*, 4076.
- (17) Stöhr, J.; Samant, M. G. *J. Electron Spectrosc. Relat. Phenom.* **1999**, *98–99*, 189.
- (18) Donald, A. M.; Windle, A. H. *Liquid Crystalline Polymers*; Cambridge University Press: Cambridge, 1992. Alexander, L. E. *X-ray Diffraction Methods in Polymer Science*; R. E. Krieger Publishing: Huntington, NY, 1979.

MA992112K